

## Studies of Terahertz Wave Propagation in Realistic Reentry Plasma Sheath

Jiamin Chen, Kai Yuan\*, Linfang Shen, Xiaohua Deng, Lujun Hong, and Ming Yao

**Abstract**—Communication ‘blackout’ is a big challenge for modern space engineering. In the recent decade, the terahertz (THz) technology is believed to be an effective solution for the ‘blackout’ problem. Many research works about the transmission of THz waves in plasma slabs have been carried out. According to those works, the radio attenuation of THz waves in plasma slabs strongly depends on thickness of the slab, electron density, electron collision frequency and temperature. However, few previous works have paid attention to realistic reentry plasma sheath. In the present paper, a hypersonic fluid model is introduced in order to investigate the structure of the realistic plasma sheath which covers a blunt coned vehicle. The scattering matrix method is employed to study the transmission of THz waves in realistic plasma sheath. According to the present study, the wave frequency, electron density and collision frequency are the most significant factors which determine the attenuation of the THz waves in the plasma sheath. Since the whole plasma sheath is inhomogeneous, to install the antenna at an appropriate position helps mitigate the ‘blackout’. For the blunt coned reentry vehicle, installing the antenna on the wall close to the bottom is helpful for mitigating the ‘blackout’ problem.

### 1. INTRODUCTION

During the hypersonic reentry stage of a space mission, the shock in front of the reentry vehicle leads to aerothermal heating on the gas around the vehicle. The neutral gas is ionized due to the high temperature. As a result, a dense plasma sheath is formed. The peak density of the plasma sheath is from  $10^{17} \text{ m}^{-3}$  to  $10^{20} \text{ m}^{-3}$  [1–3], and the corresponding cutoff frequency is in the range from 2.84 GHz to 89.8 GHz. The high dense plasma covers the whole vehicle; therefore, it shields the radio signals, and then the so-called ‘blackout’ occurs. The ‘blackout’ leads to risks on space missions and air-breathing hypersonic flights in the near space. In order to mitigate the ‘blackout’ problem, many approaches have been suggested, for example, aerodynamic shaping [4], ‘magnetic window’ [5], electrophilic ejection [6], high frequency communication and repeater satellite communication [7]. All of those approaches have technical or practical limitations, such as cost, system weight and aerodynamic performance.

For the electron density of  $10^{20} \text{ m}^{-3}$ , the cutoff frequency is 89.8 GHz, which is lower than 0.1 THz. In such a case, the terahertz (THz) solution for the ‘blackout’ problem attracts great attention in recent years. In the past decade, wireless THz communication has already come true. For example, Jastrow et al. have achieved wireless THz data transmission system operating at 0.3 THz [8]. Some researchers have started to design the THz communication system for reentry vehicles [9]. On the other hand, some other researchers tried to investigate the transmission properties of THz waves in dense plasma. By performing one-dimensional FDTD simulation, Yuan et al. analyzed the THz waves’ transmission and reflection in a hot unmagnetized plasma slab [10]. According to their study, the amplitude of transmitted THz wave is obviously modulated by the electron density profile, electron collision frequency and electron temperature. Later on, Zheng et al. investigated the THz wave transmission in dense plasma with both

---

*Received 12 June 2016, Accepted 8 September 2016, Scheduled 6 October 2016*

\* Corresponding author: Kai Yuan (y\_k\_phy@163.com).

The authors are with the Institute of Space Science and Technology, Nanchang University, Nanchang, Jiangxi 330031, China.

one-dimensional FDTD simulation and ground experiments [11]. The waves involved in the experiments were 0.22 THz. According to Zheng's study, the electron density, collision frequency and thickness of the plasma slab make significant impact on the transmission properties of 0.22 THz waves. The experiments showed that the THz technology was an effective solution for the 'blackout' problem. Moreover, the relation between the inhomogeneity of electron collision frequencies and the absorption of THz waves in plasma slab was investigated by Tian et al. [12]. They found that the inhomogeneity of the electron collision frequency in plasma sheaths significantly impacted the transmission properties of THz waves.

All of those previous studies remarkably deepen our knowledge of THz waves' transmission in reentry plasma sheaths. On the other hand, those investigations usually paid attention to the transmission of THz waves in presumed plasma slabs. In those studies, the thickness of the slab, electron density profile and electron collision frequency are usually assumed to vary independently. Unfortunately, such assumptions are not real in a realistic reentry plasma sheath. In a realistic reentry plasma sheath, the aerodynamics and hypersonic fluid dynamics dominate the spatial distribution of plasma parameters. All the plasma parameters, including electron density, temperature, electron collision frequency and thickness of the plasma sheath, vary simultaneously. Therefore, in order to find an appropriate THz approach for the 'blackout' problem, it is necessary to consider both the structure of realistic reentry plasma sheath and the transmission properties of THz waves. Such a skill has been utilized by the scientists who are interested in the 'magnetic window' approach, and they achieved noticeable success. For example, Li and Guo successfully developed a blackout prediction model based on the Navier-Stokes equations [13]. Kundrapu et al. modeled the plasma sheath of RAMC-II (Radio Attenuation Measurements C II) vehicle, and then investigated the application of the 'magnetic window' on such reentry vehicle [14, 15].

In the present paper, we first perform the numerical simulation of realistic reentry plasma sheaths based on hypersonic fluid theories. Then the transmission properties of THz waves in the plasma sheaths are investigated based on the realistic plasma sheaths obtained from the hypersonic fluid model. The scattering matrix method (SMM) is utilized for modeling the THz waves' transmission. A possible range on the wall to install the antenna is selected. The most significant factors which impact the transmission of the THz waves are investigated based on the plasma parameters near the selected range of the wall. The relation between the position of antenna and the effect of 'blackout' mitigation is discussed.

## 2. HYPERSONIC FLUID MODEL

In the present study, the reentry plasma sheath is obtained by solving a single fluid multi-species model. The model was developed by Kundrapu et al. [14, 15] based on the Navier-Stokes (N-S) equations and the gas molecular theories. The conservative form of the N-S equations is as given below:

$$\frac{\partial \rho}{\partial t} + \nabla \cdot (\rho \vec{u}) = 0 \quad (1)$$

$$\frac{\partial (\rho \vec{u})}{\partial t} + \nabla \cdot \left( \rho \vec{u} \otimes \vec{u} + p \vec{I} \right) = \nabla \cdot \vec{\tau} \quad (2)$$

$$\frac{\partial e}{\partial t} + \nabla \cdot (e \vec{u}) = -\nabla \cdot \left( p \vec{u} + \vec{q} - \vec{u} \cdot \vec{\tau} \right) \quad (3)$$

Equations (1), (2) and (3) are the mass conservation equation, momentum conservation equation and energy conservation equation, respectively. The mass density and pressure are defined as  $\rho = \sum_i^N n_i m_i$  and  $p = \rho RT$ , respectively. The viscous stress tensor is calculated according to Equation (4):

$$\vec{\tau} = -\frac{2}{3} \mu (\nabla \cdot \vec{u}) \vec{I} + \mu \left[ \nabla \otimes \vec{u} + (\nabla \otimes \vec{u})^T \right] \quad (4)$$

where superscript  $T$  is the transpose operator.

The total energy consists of thermal energy, kinetic energy of fluid and chemical energy. Therefore, the expression of the total energy is as given below:

$$e = \frac{p}{\gamma - 1} + \frac{1}{2} \rho \vec{u} \cdot \vec{u} + \sum_i^N n_i H_i \quad (5)$$

The heat flux in Equation (3) is given by the Fourier's law:

$$\vec{q} = -k_T \nabla T \equiv -c_P \frac{\mu}{Pr} \nabla T \quad (6)$$

By substituting Equation (6) into Equation (3), the energy conservation equation can be written in the form of Equation (7):

$$\frac{\partial e}{\partial t} + \nabla \cdot [\vec{u}(e + p)] = \nabla \cdot (\vec{\tau} \cdot \vec{u}) + \nabla \cdot (k_T \nabla T) \quad (7)$$

Also, the number density continuity equation is utilized in the present model:

$$\frac{\partial n_i}{\partial t} + \nabla \cdot (n_i \vec{u}) = s_i \quad (8)$$

And the rest of necessary variables are obtained from gas kinetic theories. Those expressions are given by Equations (9) to (12) [14, 16].

$$\mu_i = \frac{5}{16} \frac{\sqrt{\pi m_i k_B T}}{\pi \sigma^2 \Omega} \quad (9)$$

$$c_{P_i} = \left( \frac{f}{2} + 1 \right) R_i \quad (10)$$

$$c_{V_i} = c_{P_i} - R_i \quad (11)$$

$$k_{T_i} = \frac{5}{2} c_{V_i} \mu_i \quad (12)$$

The chemical reactions play very important role in the formation and evolution of the reentry plasma sheath. In the present model, the air 7-species model, which was developed by NASA, is introduced for the chemical reactions.  $\sigma$ ,  $\Omega$ ,  $f$ ,  $c_{P_i}$  and  $c_{V_i}$  are given by the 7-species model. Moreover, the ablation layer is taken into account in the present model although the ionization of ablation particles is ignored.

The reentry body in the present study is a blunt coned vehicle. The shape of the vehicle is identical to the vehicle of the RAMC-II experiment. The nose cap radius of the vehicle is 15.24 cm, and the half angle is 9°. The length of the vehicle is 1.29 m. The altitude of the vehicle is 31 km, and the reentry speed is 6550 m/s [17, 18].

The hypersonic fluid model is solved numerically in an unstructured mesh with finite volume method (FVM). The atmospheric condition is obtained from the NRLMSISE00 model, which is an empirical atmospheric model. The online running of the NRLMSISE00 model is available on the official website of NASA. The reentry site is assumed to be at 38.0N85.5W, which is very close to the reentry site of the RAMC-II experiment. The angle of attack is assumed to be 0° in the present study. The THz waves' transmission in the reentry plasma sheath is investigated with the SMM method based on the simulation results of the hypersonic fluid model. The SMM method will be introduced in the next section.

### 3. SCATTERING MATRIX METHOD FOR WAVE TRANSMISSION

The wavelengths of the THz waves are very small compared with both the thickness of the reentry plasma sheath and the spatial scale of the plasma inhomogeneity in the tangential direction of the plasma sheath near the wall of the vehicle. Therefore, a one-dimensional slab model is utilized to investigate the transmission properties of the THz waves in reentry plasma sheaths. The SMM method is employed to calculate the wave transmission properties. To do so, the plasma slab is divided into  $N_L$  thin layers, as illustrated in Fig. 1. The plasma parameters are homogeneous in each thin layer. The wave propagates in  $x$  direction. Region i is the free space where the wave comes from. Region ii is the plasma slab. Region iii is the free space where the antenna is located. In the present study, the antenna is settled on the wall of the vehicle. It should be noticed that the concerned waves penetrate the plasma sheath and reach the antenna. Therefore, the parameters of the slab were chosen to be the plasma parameters near the antenna.

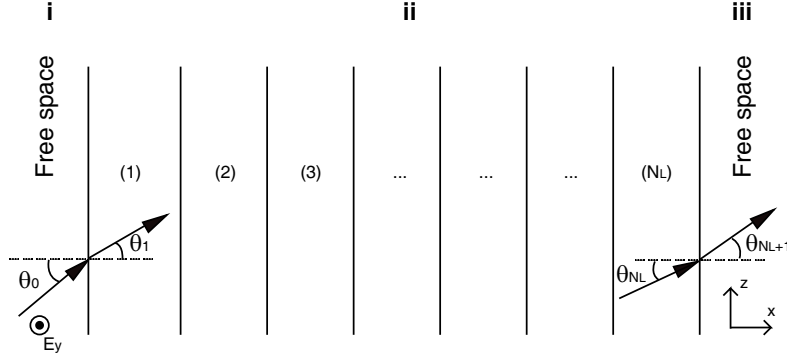


**Figure 1.** Schematic of the SMM method. The plasma slab with graded profile is divided into a number of thin layers, which are approximated as homogeneous layers with different parameters in the calculation.

**Table 1.** Nomenclature. All the variables are in SI unit system.

$\rho$ : mass density	$t$ : time	$p$ : pressure
$e$ : total energy	$n$ : number density	$m$ : mass
$R$ : gas constant	$T$ : temperature	$\mu$ : dynamic viscosity
$k_T$ : thermal conductivity	$H$ : enthalpy of formation	$\sigma$ : collision diameter
$Pr$ : Prandtl number	$s$ : source of species	$\Omega$ : collision integral
$k_B$ : Boltzmann constant	$f$ : degrees of freedom	$N$ : total number of species
$\nu_e$ : electron collision frequency	$p_0$ : standard atmospheric pressure	$c_P$ : specific heat at constant pressure
$c_V$ : specific heat at constant volume	$\gamma$ : $c_P/c_V$	$k$ : wave number
$j$ : imaginary unit	$T_g$ : global transmission coefficient	$T_p$ : power transmission coefficient
$\vec{u}$ : fluid velocity	$\vec{q}$ : heat flux	$S$ : scattering matrix
$S_g$ : global scattering matrix	$\vec{\tau}$ : viscous stress tensor	$\vec{I}$ : unit tensor

Equation (13) is the recursion formula of scattering matrix [19, 20]. The meaning of each variable is listed in Table 1.

$$S_\alpha = \frac{1}{2k_x^{(\alpha)}} \begin{bmatrix} I & III \\ II & IV \end{bmatrix} \quad (13)$$

where,

$$I = \left( k_x^{(\alpha)} + k_x^{(\alpha-1)} \right) \exp \left[ -j \left( k_x^{(\alpha-1)} - k_x^{(\alpha)} \right) d_\alpha \right] \quad (14)$$

$$II = \left( k_x^{(\alpha)} - k_x^{(\alpha-1)} \right) \exp \left[ -j \left( k_x^{(\alpha-1)} + k_x^{(\alpha)} \right) d_\alpha \right] \quad (15)$$

$$III = \left( k_x^{(\alpha)} - k_x^{(\alpha-1)} \right) \exp \left[ j \left( k_x^{(\alpha-1)} + k_x^{(\alpha)} \right) d_\alpha \right] \quad (16)$$

$$IV = \left( k_x^{(\alpha)} + k_x^{(\alpha-1)} \right) \exp \left[ j \left( k_x^{(\alpha-1)} - k_x^{(\alpha)} \right) d_\alpha \right] \quad (17)$$

and,

$$k_x^{(\alpha)} = k^{(\alpha)} \cos \theta_\alpha \quad (18)$$

In the present study, the impact led by the incident angle is not taken into account, therefore

$\theta = 0^\circ$ . In such a case,  $k_x^{(\alpha)} = k^{(\alpha)} = k^{(0)} \sqrt{\varepsilon_r^{(\alpha)}}$ . The relative permittivity is given by:

$$\varepsilon_r^{(\alpha)} = 1 - \frac{[\omega_{pe}^{(\alpha)}]^2}{\omega(\omega - j\nu_e)} \quad (19)$$

The electron collision frequency is given by:

$$\nu_e = 5.814 \times 10^{12} \frac{p}{p_0 \sqrt{T}} \quad (20)$$

which is derived based on the molecular kinetic theory and laboratory experiments by Lankford [21]. The global scattering matrix is:

$$S_g = \left( \prod_{\alpha=2}^{N_L} S_\alpha \right) \cdot S_1 \quad (21)$$

where  $S_1$  is the scattering matrix for the first layer:

$$S_1 = \frac{1}{2k^{(1)}} \begin{bmatrix} k^{(1)} - k^{(0)} & k^{(1)} + k^{(0)} \\ k^{(1)} + k^{(0)} & k^{(1)} - k^{(0)} \end{bmatrix} \quad (22)$$

Superscript 0 denotes the free space of region i. By utilizing the interface conditions for EM field on the boundaries between every two neighboring regions, a relation is obtained:

$$S_g \begin{bmatrix} R \\ 1 \end{bmatrix} = V \cdot T_g \quad (23)$$

The matrix  $V$  is defined as given below:

$$V = \frac{1}{2k^{(N_L)}} \begin{bmatrix} (k^{(N_L)} + k^{(N_L+1)}) \exp [j(k^{(N_L)} - k^{(N_L+1)}) d_{N_L+1}] \\ (k^{(N_L)} - k^{(N_L+1)}) \exp [-j(k^{(N_L)} + k^{(N_L+1)}) d_{N_L+1}] \end{bmatrix} \quad (24)$$

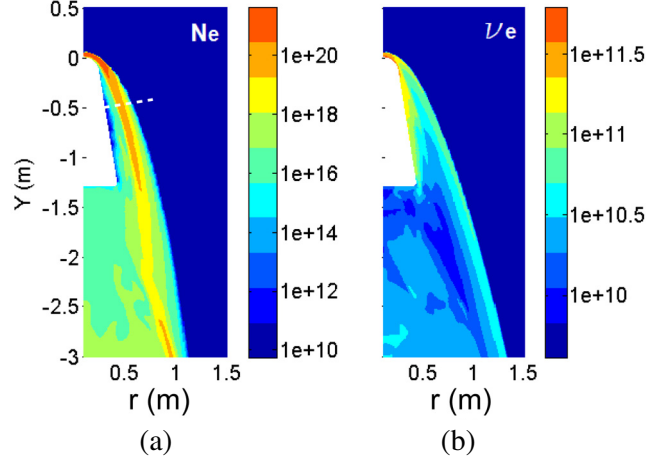
And the power transmission coefficient ( $T_p$ ) is defined as:

$$T_p = |T_g|^2 \quad (25)$$

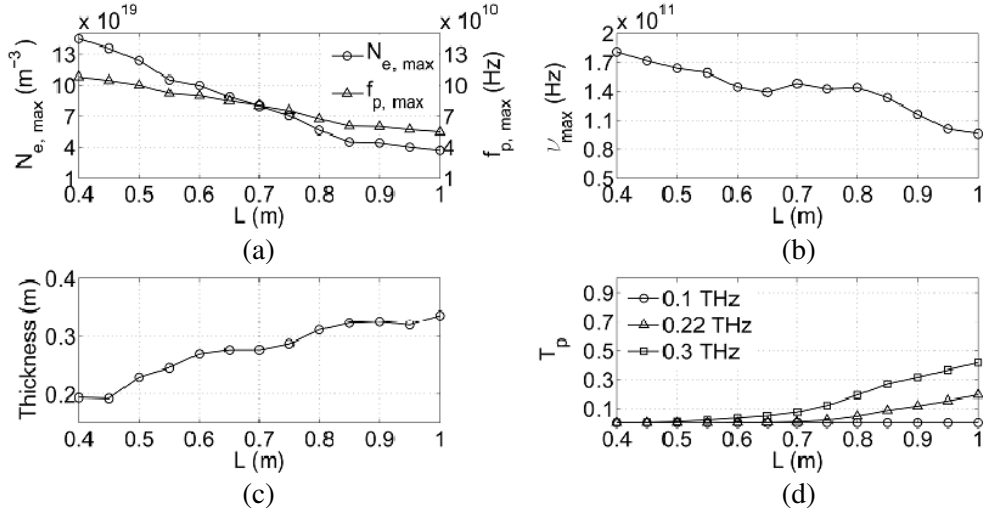
#### 4. RESULTS AND DISCUSSION

Figure 2 shows the electron density and collision frequency of the reentry plasma sheath. The reentry vehicle is an axial symmetric object, and the angle of attack is assumed to be zero. As a result, the plasma sheath is axial symmetric; therefore, only half of the whole plasma sheath is shown in the figure. In panel a, the low density area close to the wall is led by the ablation vapor. Since the ionization of the ablation component is not taken into account in the present study, the ablation vapor is completely neutral. The neutral vapor dilutes the plasma close to the wall. It is obvious that both the electron density and the collision frequency decrease with the axial distance. The thickness of the plasma sheath increases with the axial distance. The maximum electron density near the wall is nearly  $10^{21} \text{ m}^{-3}$ , and the collision frequency near the wall is nearly  $10^{11} \text{ Hz}$ . The region where the electron density is up to  $10^{21} \text{ m}^{-3}$  is very close to the nose cap of the vehicle. In the region beyond the nose cap, the magnitude of the electron density is  $10^{20} \text{ m}^{-3}$ . Fig. 3 shows more detail about the distributions of the electron density ( $N_e$ ), plasma frequency ( $f_p$ ) and collision frequency ( $\nu_e$ ) near the wall.

An area near the wall is selected in order to analyze the variation of parameters of the plasma sheath. The axial distance of the selected area is from 0.40 m to 1.0 m. In the present study, the axial distance ( $L$ ) is measured from the nose cap, at which the vertical coordinate ( $Y$ ) is 0. For each point on the wall of the vehicle,  $Y < 0$ , hence  $L = -Y$ . The antenna is assumed to be installed in a certain position on the wall in that area. The electron density, plasma frequency, collision frequency, thickness of the plasma sheath and values of  $T_p$  for the THz waves are illustrated as the functions of  $L$  in Fig. 3. Particularly, the electron density, plasma frequency and collision frequency shown in Fig. 3 are the values near the antenna. For example, the electron density at  $L = 0.50 \text{ m}$  means the average electron



**Figure 2.** The electron density and the collision frequency of the plasma sheath for the reentry speed of 6550 m/s and the altitude of 31 km. The dashed line in panel a, which is normal to the wall, indicates the main path which waves travel along.



**Figure 3.** Dependence of maximal electron density (a), collision frequency (b) and thickness (c) of the plasma sheath on the axial distance from the nose cap ( $L$ ). (d) Transmission of waves through the plasma sheath versus  $L$ .

density in the region of  $L = 0.50 \pm 0.05$  m. In panels a and b, the variable as  $N_{e,max}$  at  $L = 0.50$  m means the maximum value of  $N_e$  at  $L = 0.50$  m from the wall to the outer boundary of the plasma sheath in the region which is marked by the dashed line in panel a of Fig. 2. According to Fig. 3, the electron density decreases with  $L$ . As a result, the plasma frequency near the wall decreases with the axial distance as well. According to panel a, in the region where  $L < 0.50$  m, the plasma frequency is higher than 0.1 THz. It indicates that the waves of 0.1 THz are unable to penetrate the plasma sheath where  $L < 0.50$  m.

The electron collision frequency, which significantly impacts the energy loss of the waves [10, 11], is shown in panel b. The thickness of the plasma sheath, which impacts the transmission properties of the THz waves [11], is shown in panel c. According to panel b and panel c, the collision frequency generally decreases with  $L$ . On the other hand, the thickness of the plasma sheath increases with  $L$ . Panel d shows the values of  $T_p$  for three frequencies, which are 0.1 THz, 0.22 THz and 0.3 THz, respectively. 0.1 THz is the minimum frequency of the THz band. The waves of 0.22 THz have involved

in the ground experiments by Zheng et al. [11]. 0.3 THz has been utilized for a successful wireless THz data transmission system [8]. According to panel d, the power transmission coefficient for 0.1 THz is nearly zero over the whole selected area, although the maximum plasma frequency in the region of  $L > 0.50$  m is lower than 0.1 THz. Moreover, the plasma frequency at  $L = 1.0$  m is about 0.06 THz, which is much lower than 0.1 THz. However,  $T_p$  for 0.1 THz at  $L = 1.0$  m is still ignorable. It implies that there is significant energy loss in the transmission process even when the plasma frequency is lower than the wave frequency. Therefore, plasma density is not the sole criterion to choose the operation frequency of the communication system to solve the ‘blackout’ problem. In addition,  $T_p$  increases with the frequency of the THz waves when the frequency is higher than the maximum plasma frequency. For the frequencies of 0.22 THz and 0.3 THz,  $T_p$  increases with  $L$ . On the other hand,  $T_p$  for 0.22 THz in the region where  $L < 0.70$  m is almost ignorable, and it is smaller than 0.1 in the region where  $L < 0.85$  m. Therefore, if 0.22 THz is chosen for the operation frequency of the communication system, the antenna should be installed in the region of  $L > 0.85$  m in order to ensure that  $T_p$  is greater than 0.1 (−10 dB). For the frequency of 0.3 THz,  $T_p$  in the region of  $L < 0.50$  m is ignorable, and it is smaller than 0.1 in the region where  $L < 0.70$  m. Thus to ensure that the value of  $T_p$  for 0.3 THz is greater than 0.1, the antenna should be installed in the region of  $L > 0.70$  m.

Furthermore, according to previous studies, the attenuation of THz waves in plasma sheath increases with electron density, collision frequency and thickness of plasma sheath. However, in the case illustrated in Fig. 3, the attenuation increases with both the electron density and electron collision frequency, and decreases with the thickness of the plasma sheath. The reason is that for a given vehicle, the parameters of the plasma sheath are determined by the shape of the vehicle, reentry velocity and atmospheric condition. As a result, the electron density, collision frequency and thickness of the plasma sheath vary together. According to the numerical analysis illustrated in Fig. 3, for a given blunt coned vehicle, the electron density and collision frequency play more important roles than the thickness of the plasma sheath.

Additionally, previous studies show that the temperature influences the attenuation of THz waves in plasma sheaths [10, 11]. According to the theory by Mehra et al. [22], the radio wave attenuation in unmagnetized reentry plasma sheath is determined by the radio frequency, plasma frequency, collision frequency and length of the transmission path. Equation (19) in Section 3 shows that the collision frequency varies with the pressure and temperature. Since the collision frequency significantly impacts the attenuation of radio waves in reentry plasma sheaths, the transmission of THz waves is significantly influenced by the temperature and pressure of the plasma sheath.

In summary, according to the numerical analysis, in order to mitigate the radio communication blackout for a blunt coned reentry vehicle, the communication system should operate in THz band (0.22 THz or higher). Moreover, the most significant factors which determine the attenuation of THz waves in realistic plasma sheath are the wave frequency, electron density near the antenna and collision frequency near the antenna. Since the whole plasma sheath is inhomogeneous, installing the antenna at appropriate position helps mitigate the ‘blackout’. For a blunt coned vehicle, installing the antenna on the wall near the bottom is helpful for mitigating the ‘blackout’ problem.

## 5. SUMMARY AND CONCLUSION

In the present paper, the structure of a realistic plasma sheath which covers a blunt coned vehicle is investigated. The plasma sheath is obtained by solving a numerical hypersonic fluid model. The altitude of the vehicle is 31 km. The reentry speed is 6550 m/s, which is the same as the reentry speed of the RAMC-II experiment at 31 km. The SMM method is utilized in order to investigate the transmission of THz waves in the plasma sheath. Since the electron density and collision frequency are very high near the nose cap, a region near the wall, whose axial distance to the nose cap is from 0.4 m to 1.0 m, is selected to investigate the transmission of THz waves. Three frequencies are concerned, 0.1 THz, 0.22 THz and 0.3 THz.

According to the study, both the electron density and collision frequency decrease with the axial distance ( $L$ ) to the nose cap. On the other hand, the thickness of the plasma sheath increases with  $L$ . The power transmission coefficient ( $T_p$ ) for 0.1 THz is ignorable over the whole selected region. Therefore, the communication system should operate in the THz band, and the operation frequency

must be higher than 0.1 THz. For the waves of 0.22 THz and 0.3 THz,  $T_p$  increases with  $L$ , i.e., their attenuation increase with the electron density and collision frequency. Although the attenuation should increase with the thickness, in the present study, both  $T_p$  and thickness increase with  $L$ , i.e.,  $T_p$  increases with the thickness. The reason is that in a realistic plasma sheath of a blunt coned vehicle, the thickness of the plasma sheath is a less significant factor for the transmission of THz waves. The more significant factors are the electron density near the antenna and the collision frequency near the antenna. Moreover,  $T_p$  for 0.22 THz and 0.3 THz are greater than  $-10$  dB in the regions of  $L > 0.85$  m and  $L > 0.70$  m, respectively. In other words, in order to make sure that  $T_p$  is greater than  $-10$  dB, the communication antenna must be installed in the region of  $L > 0.85$  m when the operation frequency is 0.22 THz, or in the region of  $L > 0.70$  m when the operation frequency is 0.3 THz. In summary, the most significant factors which determine the attenuation of THz waves in a realistic plasma sheath are the wave frequency, electron density near the antenna and collision frequency near the antenna. Since the whole plasma sheath is inhomogeneous, installing the antenna at an appropriate position helps mitigate the ‘blackout’. Moreover, for a blunt coned vehicle, installing the antenna on the wall near the bottom is helpful for mitigating the communication blackout.

## ACKNOWLEDGMENT

This work was supported by the Collaborative Innovation Center of Near Space Environment and Information, Jiangxi.

## REFERENCES

1. Rybak, J. P. and R. J. Churchill, “Progress in reentry communications,” *IEEE Transactions on Aerospace Electronic Systems*, Vol. 7, No. 5, 879–894, 1971.
2. Bachynski, M., T. Johnston, and I. Shkarofsky, “Electromagnetic properties of high-temperature air,” *Proceedings of the IRE*, Vol. 48, No. 3, 347–356, 1960.
3. Leblanc, J. E. and T. Fujiwara, “Comprehensive analysis of communication with a reentry vehicle during blackout phase,” *Transactions of the Japan Society for Aeronautical and Space Sciences*, Vol. 39, No. 124, 211–221, Aug. 1996.
4. Starkey, R. P., “Hypersonic vehicle telemetry blackout analysis,” *Journal of Spacecraft and Rockets*, Vol. 52, No. 2, 426–438, 2015.
5. Hodara, H., “The use of magnetic fields in the elimination of the re-entry radio blackout,” *Proceedings of the IRE*, Vol. 49, No. 12, 1825–1830, 1961.
6. Meyer, J. W., “System and method for reducing plasma induced communication disruption utilizing electrophilic injectant and sharp reentry vehicle nose shaping,” US Patent 7237752, 2007.
7. Brandel, D. L., W. A. Watson, and A. Weinberg, “Nasa’s advanced tracking and data relay satellite system for the years 2000 and beyond,” *Proceedings of the IEEE*, Vol. 78, No. 7, 1141–1151, 1990.
8. Jastrow, C., S. Priebe, B. Spitschan, J.-M. Hartmann, M. Jacob, T. Kurner, T. Schrader, and T. Kleine-Ostmann, “Wireless digital data transmission at 300 GHz,” *Electronics Letters*, Vol. 46, No. 9, 661–663, 2010.
9. Li, J., Y. Pi, and X. Yang, “A conception on the terahertz communication system 257 for plasma sheath penetration,” *Wireless Communications and Mobile Computing*, Vol. 14, No. 13, 1252–1258, 2014.
10. Yuan, C.-X., Z.-X. Zhou, J. W. Zhang, X.-L. Xiang, F. Yue, and H.-G. Sun, “FDTD analysis of terahertz wave propagation in a high-temperature unmagnetized plasma slab,” *IEEE Transactions on Plasma Science*, Vol. 39, No. 7, 1577–1584, 2011.
11. Zheng, L., Q. Zhao, S. Liu, X. Xing, and Y. Chen, “Theoretical and experimental studies of terahertz wave propagation in unmagnetized plasma,” *Journal of Infrared, Millimeter, and Terahertz Waves*, Vol. 35, No. 2, 187–197, 2014.

12. Tian, Y., Y. Han, Y. Ling, and X. Ai, "Propagation of terahertz electromagnetic wave in plasma with inhomogeneous collision frequency," *Physics of Plasmas (1994-present)*, Vol. 21, No. 2, 023301, 2014.
13. Li, J.-T. and L.-X. Guo, "Research on electromagnetic scattering characteristics of reentry vehicles and blackout forecast model," *Journal of Electromagnetic Waves and Applications*, Vol. 26, No. 13, 1767–1778, 2012.
14. Kundrapu, M., J. Loverich, K. Beckwith, and P. Stoltz, "Electromagnetic wave propagation in the plasma layer of a reentry vehicle," *IEEE International Conference on Plasma Sciences*, 1–4, 2014.
15. Kundrapu, M., J. Loverich, K. Beckwith, P. Stoltz, A. Shashurin, and M. Keidar, "Modeling radio communication blackout and blackout mitigation in hypersonic vehicles," *Journal of Spacecraft and Rockets*, Vol. 52, No. 3, 853–862, 2015.
16. Gupta, R. N., J. M. Yos, R. A. Thompson, and K.-P. Lee, "A review of reaction rates and thermodynamic and transport properties for an 11-species air model for chemical and thermal nonequilibrium calculations to 30000 k," *NASA STI/Recon Technical Report N, Tech. Rep.*, Aug. 1990.
17. Grantham, W. L., "Flight results of a 25000-foot-per-second reentry experiment using microwave reflectometers to measure plasma electron density and standoff distance," *NASA TN D-6062*, Tech. Rep., Washington, D. C., Dec. 1970.
18. Jones, Jr., W. L. and A. E. Cross, "Electrostatic-probe measurements of plasma parameters for two reentry flight experiments at 25000 feet per second," *NASA TN D-6617*, Tech. Rep., Washington, D. C., Feb. 1972.
19. Hu, B. J., G. Wei, and S. L. Lai, "Smm analysis of reflection, absorption, and transmission from nonuniform magnetized plasma slab," *IEEE Transactions on Plasma Science*, Vol. 27, No. 4, 1131–1136, 1999.
20. Gao, P., X. Li, Y. Liu, M. Yang, and J. Li, "Plasma sheath phase fluctuation and its effect on GPS navigation," *2012 10th International Symposium on IEEE Antennas, Propagation & EM Theory (ISAPE)*, 579–582, 2012.
21. Lankford, D. W., "A study of electron collision frequency in air mixtures and turbulent boundary," *DTIC Document AFWL-TR-72-71*, Tech. Rep., Oct. 1972.
22. Mehra, N., R. K. Singh, and S. C. Bera, "Mitigation of communication blackout during re-entry using static magnetic field," *Progress In Electromagnetics Research B*, Vol. 63, 161–172, 2015.